Sindh Univ. Res. Jour. (Sci. Ser.) Vol. 45 (2) 461-466 (2013)

SINDH UNIVERSITY RESEARCH JOURNAL (SCIENCE SERIES)

Investigations of Buoyancy Effects in Sealed Rotating Cavity at different Operating Conditions

A. F. ABBASI[++], J. DAUDPOTO, S. A. SHAH, G. Y. MUGHAL

Department of Mechanical Engineering, Mehran University of Engineering and Technology Jamshoro, Sindh, Pakistan

Received 13th February 2013 and Revised 9th July 2013

Abstract: This work presents the effects of rotationally-induced buoyancy parameter on the fluid flow and heat transfer in an asymmetrical heated sealed rotating cavity system for the range of rotational Reynolds numbers$5.26\times10^5\leq Re_{\square}\leq3.11\times10^6$. These effects are predicted through the ANSYS Fluent commercial code, by adopting an axisymmetric two dimensional solver. Two turbulence models, the low Reynolds number k-ε and the Reynolds stress models are provoked for these predictions. Predictions of both the models illustrate the essential features of the heated sealed rotating cavity system. Computed flow structures show the recirculating vortices of fluid which dominated the outer part of the rotating disc space. The strength of these vortices increased at higher rotational speed. The significant effects of rotational Reynolds numbers are also observed on temperature distribution and the heat fluxes on the hot and cold disc, which are increased on the higher rotational Reynolds number. A comparison of the heat fluxes on the hot disc showed a good level of agreement with the measurements, whereas the cold disc heat fluxes are under estimated.

Keywords: Sealed rotating discs System, Reynolds stress model, k-ε model.

1. INTRODUCTION

The investigation of the fluid flow and heat transfer inside the sealed rotating cavities is of a prime interest, because these systems provide the in-depth knowledge for the gas turbine designers. Recent advancement in the gas turbine engines enhanced the scope of operating conditions that result in the amplification of the turbine entry temperature to over 1600°C as reported (Rolls-Royce, 2005). Consequently, the operating temperature of different engine components: turbine blades and nozzle guide vanes are increased which enhanced the thermal stresses and decrease the endurance period of the heat exposed parts. To enhance the turbine cycle efficiency and to devise a well-organized cooling system of the engine, a good understanding of the thermo-fluid science in a heated rotating cavity system is essential. Therefore, two methodologies are commonly used to resolve the overheating dilemma of the engine components such as the advanced composite materials and well-developed engine cooling system. Later methodology is better suited to decrease the temperature level of different components. In this state of art method, the engine cooling air is taken out from the various compressor levels. In the asymmetrical heating of the disc, the flow structure is altered due to the temperature gradient and rotationally-induced buoyancy effects. Therefore, the hot fluid is transported crossways from hot disc to the cold one, so-called axial wind (Memon, 1995). The same type transportations of the hot fluid were observed in the experimental and numerical simulations of work (Owen, *et al*., 1983), (Schiestel, *et al*., 1993) and (Gan, *et al*., 1993). Later on (Owen and Rogers, 1995) produced a monogram on the fluid flow and heat transfer behaviour in the rotating cavity system. Recently, (Randriamampianina, *et al*., 2004), (Lock, *et al*., 2005) and (Javiya, *et al.* 2012) conducted the experimental and numerical studies for the rotating disc arrangement. Overall review of previous literature pointed out that at changing rotational speed of the discs, the scenery of the flow structure in the disc cavity space is fluctuating and disordered in the nature, mainly, in the essential regions of the cavity, source and Ekman layers. To examine the fluid and heat transfer deeds in the sealed rotating cavity system, a CFD software, ANSYS Fluent has been used by selecting the turbulence models, the low Reynolds number k-ε model and the Reynolds stress model. However, the simulated results have been validated through the data of the Mark II rotating cavity rig at the TFMRC University of Sussex (Memon, 1995).

2. NUMERICAL METHOD

The simple geometry of the sealed cavity system is presented in **(Fig. 1)**. The geometric dimensions and operating conditions ($5.26\times10^5\leq Re_{\square}\leq3.11\times10^6$ and $C_w=0$) are identical to the experimental rig as under,

b=427.5mm, s=56.0mm and G=s/b=0.138

[++]Corresponding author: Email: afateh66@yahoo.comCell. No. +92-3793045

The temperature distribution on the hot disc is supposed to be non-uniform and increasing with the radius of the disc and reached higher level of 100°C at external edge of the disc, whereas, temperature of the cold disc is fixed at 20°C.The flow boundary conditions at the inlet and outlet was set to zero, because of no mass flow rate. A non-uniform meshing arrangement of 75×92 in axial and radial directions respectively have been adopted with a closest off-wall node distance $y^+ < 0.5$ to ensure the fine distribution of the nodes in the near-wall region, as shown in **(Fig.2)**. To evaluate the unknown variables at control volume faces, the HYBRID and HOUS discretisation schemes have been adopted in combined form for the mean and fluctuating components respectively. To update the pressure field, correct the velocity values and satisfy the mass continuity of flow, the SIMPLEC algorithm of (Van Doormal and Raithby, 1984) has been employed.

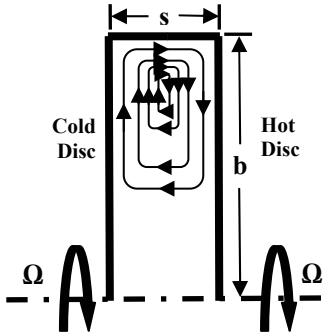

Fig. 1. Schematic diagram for Sealed rotating cavity system

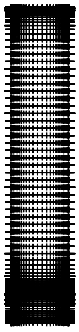

Fig. 2. Non-uniform grid arrangement

3. TURBULENCE MODELS

The energy equation activated along with the two turbulence models, the low Reynolds number k-ε model and the Reynolds stress model. These models are available by default in the ANSYS Fluent CFD code. Both the turbulence models are categorised according to the modelling of the Reynolds stress components, which are appeared in the time-averaging process of a Navier stokes equations. The details of governing equations are given as,

3.1 Low Reynolds number k-ε model

In the first step, a mean flow closure (low Reynolds number k-ε model) of (Morse, 1991) has been used. In this modelling procedure turbulent quantities are resolved by the gradient transport hypothesis method, which is based on the transport equation for the kinetic energy (k) and its dissipation rate (ε).

$$\rho\overline{u_i u_j} = 2/3\delta_{ij}\rho k - \mu_T\left(\frac{\partial U_i}{\partial x_j} + \frac{\partial U_j}{\partial x_i} - 2/3\,\delta_{ij}\nabla.\underline{V}\right) \quad (1)$$

where $\nabla.\underline{V}$ is the divergence of the velocity vector,

$$\nabla.\underline{V} = \frac{\partial U}{\partial z} + \frac{\partial V}{\partial r} + \frac{V}{r} \quad (2)$$

$2/3\,\delta_{ij}$ = Normal stresses (i.e. i=j only)

3.2 Reynolds Stress model

In second step, the Reynolds stress model, which is based on the recommendations of (Lai and So, 1990) has been used for the simulations. In this modelling process, an isotropic eddy viscosity technique is not applied and the transport equations are resolved for each Reynolds stress component so-called Reynolds stress closure. The exact equation for the Reynolds stress components are presented in Cartesian tensor as

$$\frac{\partial}{\partial x_k}\left(\rho U_k\overline{u_i u_j}\right) = \frac{\partial}{\partial x_k}\left(\mu\frac{\partial\overline{u_i u_j}}{\partial x_k}\right) + \frac{\partial}{\partial x_k}\left(-\rho\overline{u_i u_j u_k}\right) - \rho\left(\overline{u_j u_k}\frac{\partial U_i}{\partial x_k} + \overline{u_i u_k}\frac{\partial U_j}{\partial x_k}\right) - \overline{\left(u_i\frac{\partial p}{\partial x_j} + u_j\frac{\partial p}{\partial x_i}\right)} - 2\mu\overline{\frac{\partial u_i}{\partial x_k}\frac{\partial u_j}{\partial x_k}} \quad (3)$$

or symbolically as

$$C_{ij} = D^{\nu}_{ij} + D^{T}_{ij} + P_{ij} + \Pi_{ij} - \varepsilon_{ij} \quad (4)$$

where from left to the right can be read as convection, viscous diffusion, turbulent diffusion, production by mean strain, redistribution and diffusion due to the pressure interactions, and viscous dissipation of the Reynolds stresses respectively. For full detail see references, (Abbasi *et al.,* 2012), (Memon, 1995 and 1999) and (Lai and So, 1990).

3.3 Energy equation

The generalized form of the Reynolds-averaged energy equation for steady turbulent flow can be written in Cartesian tensor notation as,

$$\frac{\partial}{\partial xj}(Uj\ \phi) = \frac{\partial}{\partial xj}\left[\frac{\mu}{\Pr}\frac{\partial\phi}{\partial xj} - \overline{uj\ \phi}\right] \quad (5)$$

For the cylindrical polar-coordinate system:

$$\frac{\partial}{\partial x}(U\phi)+\frac{1}{r}\frac{\partial}{\partial r}(rV\phi)=\frac{\partial}{\partial x}\left(\frac{\mu}{\Pr}\frac{\partial\phi}{\partial x}\right)+\frac{1}{r}\frac{\partial}{\partial r}\left(\frac{r\mu}{\Pr}\frac{\partial\phi}{\partial r}\right)+S_{\phi} \quad (6)$$

Where the turbulent heat flux tensor emerged in equation (5) is represented by the source term (S_{ϕ}).

4. DISCUSSION OF NUMERICAL RESULTS

This section presents the fluid flow and heat transfer predictions for a closed rotating cavity system for the varying values of rotational Reynolds numbers, $5.26\times10^5\leq Re_{\square}\leq3.11\times10^6$ and without mass flow rate, $C_w=0$. These operating conditions are same as used in the experimental work.

4.1 Computed stream lines

(Fig.3a-c) illustrates the comparison of the simulated stream lines for a range of rotational Reynolds number, $5.26\times10^5\leq Re_{\square}\leq3.11\times10^6$. For lower rotational speed, $Re_{\square}=5.26\times10^5$ both the models predicted the recirculating cell of air in the outer part of the cavity. Result of that, the hot fluid is transported to the cold one, as shown in **(Fig. 3a)**. For higher rotational speed, $Re_{\square}=1.70\times10^6$, rotationally-induced buoyancy effects are dominant; consequently the size of recirculating cell is contracted, as shown in **(Fig.3b)**. For the maximum rotational speed, $Re_{\square}=3.11\times10^6$, the recirculating cell of the fluid is further contracted in the same manner and formed a double recirculating cells of fluid in outer part of the cavity, as illustrated in **(Fig.3c)**. These recirculating cells of fluid indicated that the higher rotational speed of two discs produced the centrifugal force across the two discs, which enhanced the rotationally-induced buoyancy force. This force pushes the air in the outward direction and returns back inward direction along the hot disc then moves axially to the cold disc. Result of that, recirculating cells of the fluid are developed in external region of the cavity. The comparison two models demonstrated that the Reynolds stress model predicted extra compressed cell than that of the k-ε model particularly at higher rotational speed. This attributes that the former model captured the turbulent flow situation more appropriately.

4.2 Simulated static temperature contours

(Fig.4a-c) illustrates the static temperature contours for the same range of rotational Reynolds number, $5.26\times10^5\leq Re_{\square}\leq3.11\times10^6$. The significant effects of the rotationally-induced buoyancy parameter are also observed on the temperature distribution. These effects reveals that the recirculating flow on the hot disc does not annulled out because of no mass flow and formed the recirculating cell of fluid. Result of that heat transfer in the cavity is influenced by free convection instead of forced convection. For the case of lower value of Reynolds number, $Re_{\square}=5.26\times10^5$, the temperature distribution shows the larger recirculation of fluid between the discs. Consequently, the temperature distribution starts from earlier stage of the cavity as illustrated in **(Fig.4a)**. For higher rotational speed, $Re_{\square}=1.7\times10^6$ the static temperature contours show the temperature distribution in the outer part of the cavity, as shown in **(Fig.4b)** this signifies the fluid cell contraction at higher rotational speed (see Fig.3c). For the highest rotational speed, $Re_{\square}=3.11\times10^6$ the strong axial wind of the air is formed between the two discs which carry the hot fluid from the hot disc to the cold disc, consequently a higher temperature distribution takes place within the two disc space, as shown in **(Fig.4c)** .

4.3 Computed heat flux

In the sealed rotating cavity there is no inflow of the mass. Therefore, the inlet temperature condition cannot be defined appropriately; thus the fluid properties are described on the bases of radially-weighted cold-disc average temperature (Memon, *et al.*, 2002). Similarly, the local Nusselt numbers cannot be calculated correctly due to unavailability of fluid temperature. Thus the heat transfer calculations are presented through dimensional heat fluxes (W/m^2). Due to zero mass flow rate, the radiative effects are very important for the heat transfer calculations. To analyse the vital effects of the radiative components, the total heat fluxes (i.e.$q_t=q_r+q_c$) are considered here for heat transfer calculations. Because these heat fluxes are helpful for mimic the correct behavior of heat transfer than that of the convective heat transfer. However, comparison have been made among the simulations and measurements for both the heat fluxes, convective and total (total=convection+radiation). **(Fig.5a-c)** illustrates cold disc heat fluxes for the range of rotational Reynolds number $5.26\times10^5\leq Re_{\square}\leq3.11\times10^6$. All the predicted heat fluxes showed negative profiles in the outer part of the cavity, mainly total heat fluxes showed extra negative levels than convective one. This signifies the consideration of radiative heat effects in the total heat fluxes. The computation and measurements shows that the value of negative fluxes amplified in radial direction, which revealed that the axial temperature difference increased with the radius because of recirculating hot fluid. (Memon, 1995) also mentioned that the heat inflow to the cold disc increased with radius, consequently the axial temperature differences increased with the same manner. For higher rotational speed, $Re_{\square}=1.70\times10^6$and 3.11×10^6 the strength of recirculating vortex are increased, which affect the transportation of heat from the hot disc to the cold one. Therefore, higher value of negative heat fluxes has been simulated for the colder disc. The assessment of result of two turbulence models showed the same trends of variation in heat fluxes in all the flow regions of the cavity. A comparison of the heat fluxes

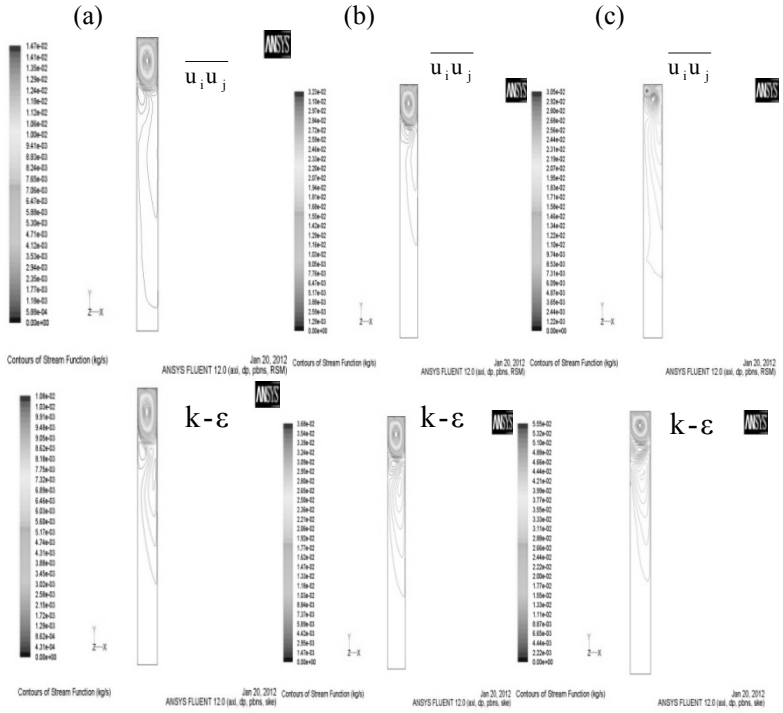

Fig. 3. Comparison of computed flow structures for $5.26\times10^5 \leq Re_{\square} \leq 3.11\times10^6$ and $C_w = 0$

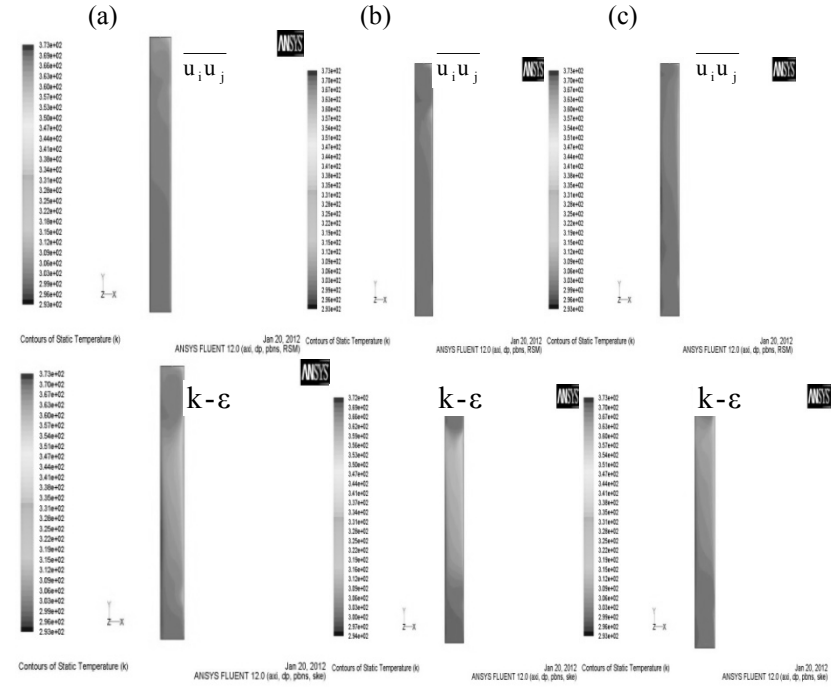

Fig. 4.Comparison of computed static temperature for $5.26\times10^5 \leq Re_{\square} \leq 3.11\times10^6$ and $C_w = 0$

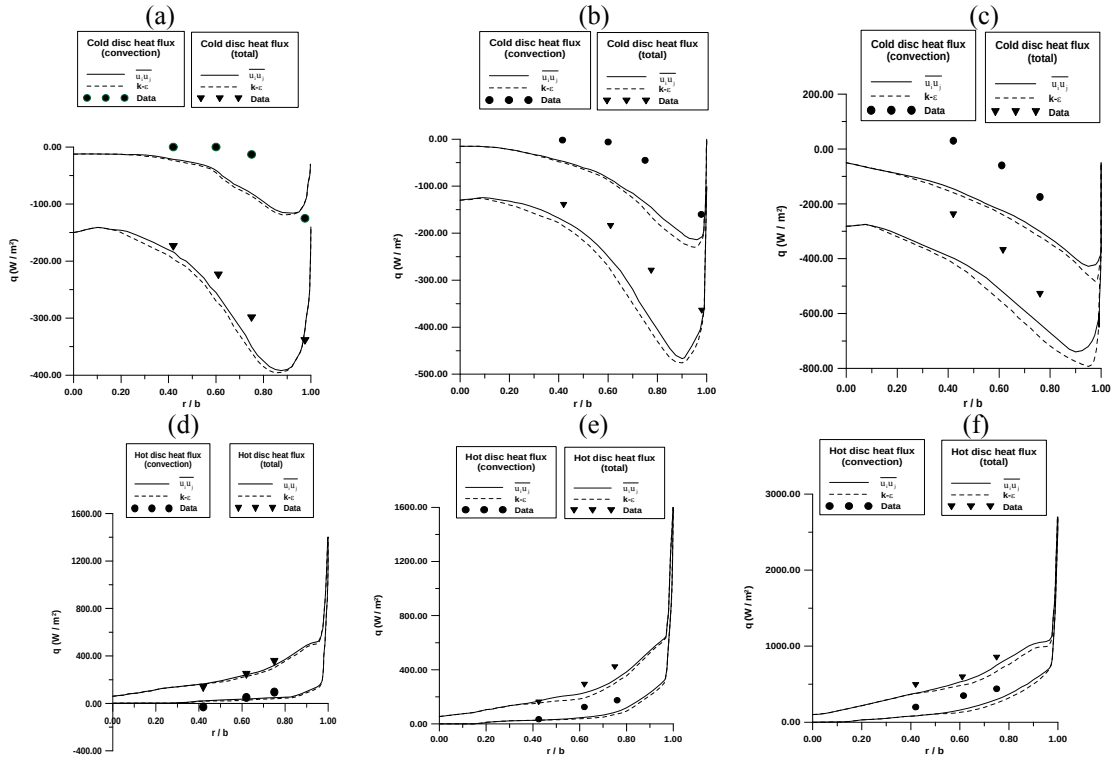

Fig. 5. Comparison of cold disc and hot disc heat fluxes (convection and total) for sealed rotating cavity for $5.26\times10^5 \leq Re_{\square} \leq 3.11\times10^6$ and $C_w = 0$

(convection and total) illustrates that simulations underestimated the measurements in the central region; however, the Reynolds stress model presents a slightly closer matching with the experimental data.

(Fig.5d-f) presents the hot disc heat fluxes, for the same range of rotational Reynolds number $5.26\times10^5 \leq Re_{\square} \leq 3.11\times10^6$. The comparisons of simulations and measurements show that the convective heat fluxes amplified due to higher rotational speed. For the lowest rotational speed, $Re_{\square}=5.26\times10^5$ the convective heat fluxes are almost zero at the lower radial location, r/b=0.3, as this is limited to r/b=0.15 for the highest rotational speed, $Re_{\square} =3.11\times10^6$. For this highest rotational speed, there is rapid increase in the heat fluxes, which shows the strong influence of the buoyancy induced parameter. Similarly, level of total heat fluxes influences by the buoyancy induced parameter. Comparison of both the heat fluxes show that the total heat fluxes showed higher level than that of the convective heat fluxes. The level of these heat fluxes are amplified with radius and abruptly increased in the outer region. This abrupt increase in the heat flux signifies the higher temperature distribution in the outer area of the disc. The evaluation of predictions and measurements shows that the Reynolds stress model shows a nearer agreement with the measurements than that of the low Reynolds number k-ε model.

5. CONCLUSIONS

An asymmetrical heated sealed rotating cavity system has been examined for the varying rotational speeds. An increase in the rotational speed increased the rotationally-induced buoyancy parameter which is characterised by an increase in the strength of the recirculating vortex; consequently heat is transferred from the hot disc to the fluid and than to the cold disc. The influence of radiative heat transfer is also significant in asymmetrically heated sealed cavity. Present computational results confirmed the influence of the radiative heat parameter on the overall heat transfer calculations. Predictions indicated the negative heat fluxes for the cold disc, which signified the recirculation effects on the heat fluxes. The overall comparison between the predictions and measurements shows that the predicted heat fluxes were under predicted than the measurement. This discrepancy may be attributed towards an axial inlet gap that actually used in the superimposed radial outflow for the incoming fluid, was left open in the corresponding experimental work for a sealed cavity flow (Memon,1995). Thus, the exit of hot fluid from the cavity and an admission of the cooling fluid in the cavity may result in the higher heat transfer rates for the hot disc and the lower heat inflow to the cold disc.

ACKNOWLEDGEMENTS

The authors would like to acknowledge this work to Higher Education Commission, Ministry of Science and Technology Government of Pakistan for providing an opportunity and financial support to fulfil this work. Authors are also thankful to the Mehran University of Engineering and Technology and Faculty members Department of Mechanical Engineering for their encouragement and moral support.

NOMENCLATURE

b	outer radius of cavity
$C_w = \dot{m}/\mu b$	non-dimensional mass flow rate
G = s/b	cavity gap ratio
k	turbulent kinetic energy
p	static pressure
Pr	Prandtl number
q	heat flux
$Re_\theta = \Omega b^2/\nu$	rotational Reynolds number
r	radial co-ordinate
r/b	non-dimensional radial co-ordinate
r_i	inner disc radius
S	source term
s	axial gap between the discs
U,V,W	mean velocity components in z, r, θ
u,v,w	fluctuating velocity components in z, r, θ
$\overline{u_i u_j}$	Reynolds stress tensor
$y^+ = y u_\tau/\nu$	wall-distance Reynolds number
z	axial co-ordinate
z/s	non-dimensional axial co-ordinate
ε	dissipation rate of turbulent kinetic energy
μ	dynamic viscosity
μ_T	turbulent viscosity
ϕ	generalised transport variable
Ω	rotational speed of the disc
ρ	density
δ_{ij}	Kronecker delta

REFERENCES:

Abbasi, A. F., M. D. Memon, and A. Baloch, (2012) Modelling and predictions of isothermal flow Inside the closed rotor-stator flows. Mehran University Research Journal of Engineering & Technology. 31(1): 83-94.

Gan, X., M. Kilic, and J. M. Owen, (1993) Flow and heat transfer between gas turbine discs. AGARD-CP-527, 25.1-25.11.

Javiya, U., J. W. Chew, N. J. Hills, L. Zhou, M. Wilson, and G. D. Lock, (2012) CFD analysis of flow and heat transfer in a direct transfer preswirl system. J. Turbomachinery.

Lai, Y. G. and R. M. C. So, (1990) On near-wall turbulent flow modelling. J. Fluid Mech. 221: 641-673.

Lock, G. D., Y. Youyou, P. J. Newton, M. Wilson, and J. M. Owen, (2005) Heat transfer measurements using liquid crystal in a pre-swirl rotating-disc system. J. Turbomachinery. 127: 375-381.

Memon, M. D. (1995) Numerical modelling and prediction of fluid flow and heat transfer in rotating disc geometries. D.Phil. Thesis, University of Sussex.

Memon, M. D., A. A. Memon, and M. H. Jokhio, (1999) Application of the low Reynolds number second moment closure to the closed rotor-stator flows. Mehran University Research Journal of Engineering & Technology. 18 **(2)**:117-121.

Memon, M. D. and M. A. Uqaili, (2002) Computation of fluid flow and heat transfer in sealed rotating cavity. Mehran University Research Journal of Engineering & Technology. 21**(2)**: 97-108.

Morse, A.P. (1991) Application of a low Reynolds number k-ε turbulence model to high-speed rotating cavity flows. J. Turbomachinery. 113: 98-105.

Owen J. M. and R. H. Rogers (1995) Rotating cavities, Flow and Heat Transfer in Rotating Disc Systems 2, Rotating cavities. Research Studies Press/John Wiley Inc. New York.

Owen, J. M. and H. S. Onur, (1983) Convective heat transfer in a rotating cylindrical cavity. J. Eng. Pwr.105: 265-276.

Randriamampianina, A., R Schiestel, and M. Wilson, (2004) The turbulent flow in an enclosed corotating disk pair: axisymmetric numerical simulation and Reynolds stress modelling. Int. J. Heat and Fluid Flow. 25: 897-914.

Rolls-Royce (2005) The Jet Engine, Rolls-Royce Publications.

Van Doormal, J. P. and G. D. Raithby, (1984) Enhancement of the SIMPLE method for predicting incompressible fluid flow. Num. Heat Transfer. 7: 147-163.